HHS Public Access

Author manuscript

Macromol Biosci. Author manuscript; available in PMC 2019 February 01.

Published in final edited form as:

Macromol Biosci. 2018 February ; 18(2): . doi:10.1002/mabi.201700263.

Micro-Nanostructures of Cellulose-Collagen for Critical Sized Bone Defect Healing[a]

Aja Aravamudhan,
Skeletal Cranial Biology, UConn Health, Farmington, CT-06030, US

Daisy M. Ramos,
Materials Science and Engineering, University of Connecticut, Storrs, CT-06269, US

Jonathan Nip,
Department of Biomedical Engineering, University of Connecticut, Storrs, CT-06269, US

Ivo Kalajzic [Professor], and
Department of Reconstructive Sciences, Uconn Health, Farmington, CT-06030, US

Sangamesh G. Kumbar* **[Professor]**
Skeletal Cranial Biology, UConn Health, Farmington, CT-06030, US

Materials Science and Engineering, University of Connecticut, Storrs, CT-06269, US

Department of Biomedical Engineering, University of Connecticut, Storrs, CT-06269, US

Department of Orthopaedics, UConn Health, Farmington, CT-06030, US

Abstract

Bone tissue engineering (BTE) strategies utilize biodegradable polymeric matrices alone or in combination with cells and factors to provide mechanical support to bone, while promoting cell proliferation, differentiation, and tissue ingrowth. The performance of mechanically competent, micro-nanostructured polymeric matrices, in combination with bone marrow stromal cells (BMSCs), was evaluated in a critical sized bone defect. Cellulose acetate (CA) was used to fabricate a porous micro-structured matrix. Type I collagen was then allowed to self-assemble on these micro-structures to create a natural polymer-based, micro-nanostructured matrix (CAc). Poly (lactic-co-glycolic acid) (PLGA) matrices with identical micro-structures served as controls. Significantly higher number of implanted host cells were distributed in the natural polymer based micro-nanostructures with greater bone density and more uniform cell distribution. Additionally, a two-fold increase in collagen content was observed with natural polymer based scaffolds. This study establishes the benefits of natural polymer derived micro-nanostructures in combination with donor derived BMSCs to repair and regenerate critical sized bone defects. Natural polymer based materials with mechanically competent micro-nanostructures may serve as an alternative material platform for bone regeneration.

TOC image

[a]Supporting Information is available online from the Wiley Online Library or from the author.

Professor Sangamesh G. Kumbar: kumbar@uchc.edu.

Micro-nanostructures of cellulose and collagen (CAc) were prepared and their ability to regenerate a critical sized bone defect was evaluated. When donor derived BMSCs were used in combination with the CAc structures in mice, a significant bridging of the defect was seen. Also, twice as much collagen and bone density was seen in the regenerated bone in contrast to the regeneration achieved by synthetic polymer. This preclinical study indicates the potential of cellulose-collagen micro-nanostructures to be an alternative BTE material to the conventional polyester based materials.

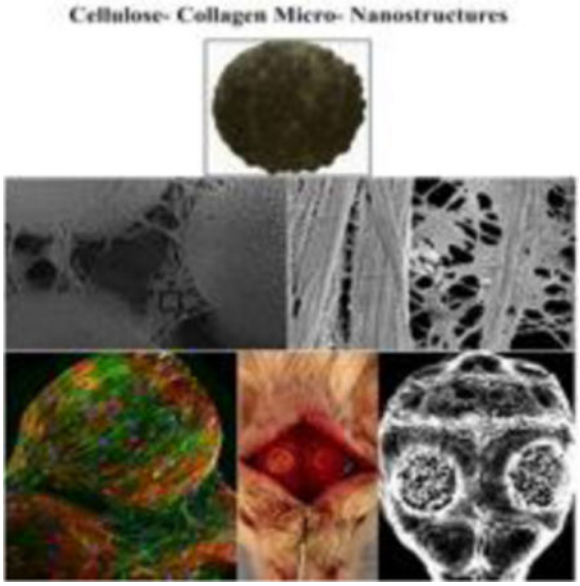

Keywords

TISSUE ENGINEERING; MICRO-NANOSTRUCTURES; BONE; STEM CELLS; REGENERATION

1. Introduction

Bone represents one of the most transplanted organs with roughly 500,000 bone grafts implanted annually in the U.S.[1]. Though autografts, patient's own bone, are considered the gold standard for achieving bone healing, they are restricted by availability and bring additional discomfort to patients. Allografts, bone taken from cadavers, overcome these limitations, but display low remodeling due to excessive processing of the allogenic material, and carry the risk of disease transmission [2]. Bone tissue engineering provides an alternative treatment, where biomaterial matrices, biological factors, and cells are used alone or in combination for enhanced bone regeneration [2].

Tissue engineered matrices act as templates for regeneration to occur and the properties of the biomaterial can dictate the nature and quality of the regenerated bone[3]. It is well known that material properties such as hydrophilicity[4], morphology[5] and mechanical properties[6] can be used to directly enhance bone healing. Several polymeric materials, such as poly-L-lactide (PLLA) and poly (lactic-co-glycolic acid) (PLGA) are commonly used in

the formulation of scaffolds for bone regeneration[7]. Though, synthetic polymers lend themselves to be readily tunable to obtain desired mechanical and degradation properties, concerns are raised due to their highly hydrophobic nature and acidic bulk degradation products[8, 9].

Polymers of natural origin such as polysaccharides and proteins are synthesized in biological systems like plants, animals, and microbes and therefore have structures similar to the extracellular matrix (ECM) macromolecules seen in the body[10]. Hence natural polymers have a higher degree of biomimicry and offer greater biocompatibility in tissue healing[11, 12]. Though a number of attempts have been made to create systems with natural and synthetic components[13], very few successful efforts have been made towards the design of an all-natural based system that provides adequate functions of mechanical competence, porosity and bioactivity[14]. For example, collagen[15], polysaccharides like chitosan[11],[16], and protein based structures are often presented in the form of porous sponges, fiber matrices or hydrogels, which lack mechanical stability and require chemical crosslinking to produce stable structures. Additionally, during fabrication, extensive processing and crosslinking can compromise the biological functionality of these systems[17]. Previously, we have successfully developed a mechanically competent micro-nanostructured polymeric system[18] with increased bioactivity[19] for bone tissue engineering. We followed a two-pronged approach by designing a mechanically competent, 3D sintered microsphere porous base, made of cellulose acetate (CA), which is further functionalized with self-assembled nanofibrillar collagen (CAc)[18, 19]. The cellulose materials allowed greater biomimetic self-assembly of collagen nanofibers over PLGA resulting in greater osteoinductivity of human mesenchymal stem cells (hMSCs), *in vitro*. The cellulose materials also showed greater biocompatibility compared to PLGA in a subcutaneous rodent model[20].

Often times, the inclusion of factors or stem cells is needed to achieve complete tissue regeneration. In such cases, the biomaterial scaffold can act as both a template matrix and a factor delivery vehicle[21]. While the delivery of growth factors such as BMPs has had mixed outcomes, such as ectopic bone formation[22], a clinically viable alternative is the use of autologous bone marrow stromal cells (BMSCs)[23]. In addition to being a cell delivery vehicle, the scaffold acts as an instructive temporary ECM to control and direct the survival, proliferation and differentiation of stem cells and ultimately dictate the quality of regenerated bone[24, 25]. Hence the mechanical, pore properties, chemical functionalities, and nanoscale topographical features[6, 26] can all influence the osteogenic differentiation of BMSCs. Few studies however do not examine the role of these material characteristics towards regeneration *in vivo* when combined with BMSCs.

In this study, we contrasted the *in vivo* performance of natural polymer based (CA and CAc) micro-nanostructured matrices against the performance of well-established synthetic polymeric (PLGA) matrices of the same architecture[18, 19, 27, 28]. Our previous work had shown greater osteoconductive, and osteoinductive nature of the cellulose-collagen system *in vitro* and greater biocompatibility of the matrices over PLGA, *in vivo*, in a subcutaneous implant rat model[19, 20]. It was hypothesized that the natural micro-nanostructured matrices, due to greater biocompatibility, would be more conducive for cellular infiltration.

Additionally, it was hypothesized that the natural micro-nanostructured matrices would offer greater osteoinductive environments for donor BMSCs, leading to superior bone formation.

2. Experimental Section

2.1. Materials

Cellulose acetate (Mw: 30K) (CA), and Polyvinyl Alcohol (30,000-70,000) (PVA) were procured from Sigma -Aldrich (St. Louis, MO, USA). Poly(lactic-co-glycolic acid) 85:15 (PLGA) was purchased from lakeshore biomaterials (Birmingham, USA). Acetone, dichloromethane, cyclohaxane, paraformaldehyde, and gluteraldehyde were purchased from Fisher Scientific (Fair Lawn, NJ, USA).

2.2. Preparation of microspheres

Oil in water solvent-evaporation, followed by sintering of formed microspheres using a solvent/non-solvent mixture was used for producing microsphere of i) Cellulose acetate (CA), ii) poly (lactic-co-glycolic acid) 85:15 (PLGA). In brief, 13(w/v)% of CA polymer was dissolved in a solvent mixture containing methylene chloride and acetone at a ratio of 9:1 to produce microspheres. A 20(w/v)% solution in methylene chloride was used in the case of PLGA polymer to produce the microspheres. The polymer solutions were then poured in a thin stream into an aqueous media containing 1.25(w/v)% PVA as a surfactant, with constant stirring at 250rpm to form an oil-in-water emulsion. These suspensions were stirred overnight to evaporate the solvent to obtain hardened microspheres. Isolated microspheres were washed repeatedly with deionized (DI) water, dried, and sieved into different microsphere sizes. Microspheres in the size range of 200-425μm were sintered into micro porous scaffolds using either solvent-non-solvent or heat sintering based on the polymer[18, 19].

2.3. Preparation of micro-porous sintered 3D microsphere matrices

Metal molds were filled with CA microspheres to which a 200μL volume of an optimized solvent/non-solvent composition, acetone: cyclohexane in the ratio of 3:1 (v/v), was added to cover the microspheres. Solvent was allowed to evaporate at room temperature to obtain sintered microsphere scaffolds. Cylindrical scaffolds measuring 3.5mm diameter X 1mm height were used for implantation into mouse calvaria. The control PLGA micro porous scaffolds with identical micro-particle sizes were heat sintered at 95°C for 45 minutes[18]. The volume of the microsphere mold was 9.6mm^3.

2.4. Preparation of collagen nanofiber infused cellulosic 3D microporous matrices

A modified biomimetic approach was used to functionalize micro porous scaffolds with type I collagen. In brief, the test CA scaffolds were incubated in a 0.1(w/v)% collagen type I solution (pH adjusted to 4.2) at 37°C for 7 days to promote molecular collagen self-assembly. The dried scaffolds were treated with UV light for 30 min each side to achieve collagen nanofiber stability and washed repeatedly with DI water to remove buffer salts[19].

2.5. Characterization of internal structure of scaffolds by SEM

Scanning electron microscopy (SEM) was used to characterize scaffold morphology and evaluate collagen fiber diameter and distribution. Scaffolds were sputter coated with Au/Pd using a Polaron E5100 sputtering system (Quorum Technologies, East Sussex, UK) to achieve an eighteen-nanometer thick coating before viewing under SEM. The samples were viewed using FEI Nova NanoSEM 450 scanning electron microscope (FEI, Hillsboro, OR, USA) operated at an accelerating voltage of 2kV at various magnifications.

2.6. Transgenic models

We have utilized previously described transgenic models in which a fragment of type I collagen promoter (Col3.6kb) directs the expression of green fluorescent marker (GFP) to osteoblast lineage cells. Green (Col3.6tpz) and cyan (Col3.6cyan) variants were used[29].

2.7. Design of calvarial implantation studies

All animal procedures were approved by the Institutional Animal Care and Use Committee (IACUC) at the University of Connecticut Health Center and all efforts were made to minimize animal suffering. CD-1 wild type female mice (10-12 weeks old), weighing 26-32 g were used for implantation of the scaffolds alone. Cell-seeded matrices were implanted into male Col3.6tpz that were bred into NOD scid gamma immunodeficient background (jax stock Stock No:005557 |NSG) (10-12 weeks old), weighing 25-30g. Donor cells were obtained from Col3.6cyan transgenic mice. Thus, the fluorescent reporters acted as a tool to determine the quantity of active osteoblasts formed by the donor cells and the host cells. In the study with materials alone an n=6 was used, while an n=24 was used in the case of cell seeded constructs. Each scaffold was sterilized by soaking in 70% ethanol followed by UV treatment for 20 minutes on each side. Matrices were washed with sterile PBS and either directly implanted or implanted after seeding donor cells as described below[30]. The samples were retrieved at 8 weeks for radiological and histological examination.

2.8. BMSC Culture

The tibia and femur of 6-8 week old Col3.6cyan mice were isolated and the epiphyses were removed. Media (α-MEM) containing 1% Penicillin/Streptomycin and 10% FBS was used to flush the bone marrow. The flushed cells were filtered with a 70μm cell strainer and centrifuged for ten minutes at 350×g. The pelleted cells were resuspended in media and plated at a density of 3×10^6 cells/cm^2. A 50% media change was completed at day 4 of culture, followed by full media change after 7 days. Once confluent at day 10, cells were lifted with Trypsin EDTA (2.5%) solution and suspended in media with serum to achieve a cellular concentration of 1×10^6 cells/mL for implantation[31].

2.9. Calvarial surgery

A combination of Ketamine (135 mg/kg) and Xylazine (15 mg/kg) was administered (I.P.) to anesthetize the mice (CD-1 wild type mice for implantation of scaffold alone and Col3.6tpz mice in the case of BMSC seeded scaffolds). An incision was made to expose the cranium and a 3.5mm critical sized defect was made on each side, using a drill bit, taking care that the underlying dura matter was not damaged as illustrated in Figure 1A. A two-hole mouse

calvarial model was used and the scaffolds were placed into theses defects as per the study design (Figure 1B)[25]. In the case of cell-seeded matrices, 1×10^6 cells (Col3.6Cyan) BMSCs were seeded onto the matrices. 1×10^6 cells (Col3.6Cyan) BMSCs were spun down to create a pellete with minimal amounts of media. This pellete was mechanically transferred onto the PLGA/CA/CAc structures by using a micropipette, making sure all the cells were transferred onto the scaffolds. These scaffolds were then used for implantation into mouse calvarial defects.

3. Results

3.1. Scaffold Morphology

The appearance of synthesized PLGA, CA and CAc materials were examined using a dissection microscope and their internal structure was analyzed by scanning electron microscopy (SEM). The 3D porous structures of PLGA were golden in color (Figure 2A), while CA (Figure 2B) and CAc (Figure 2C) were opaque and white in color. Under high magnification with SEM, PLGA 3D porous materials (Figure 2 D, G, J) showed a smooth surface morphology (arrows), whereas CA (Figure 2 E, H, K) showed many surface undulations (arrows), depicting a rougher surface associated with CA structures. Collagen nanofibers self-assembled on the CA microspheres in CAc (Figure 2 F, I, L) and formed a uniform coating on the microsphere without accumulating at the pores of the material (arrows). These structural features prove that CA presents a less smooth surface and allowed for uniform collagen nanofiber assembly.

3.2. Radiological examination of bone formation

At 8-weeks post implantation, the animals were sacrificed and the calvarias were dissected and removed (Supplemental Figure S1-A, B, C in the case of unseeded materials and Figure 3A-1,2,3 in the case of materials seeded with BMSCs). X-ray was used to evaluate the amount of bone formation in the materials. The radiopacity of the tissue formed in the case of implants alone was minimum and mostly represented a background signal (Supplemental Figure S1-D, E and F). However, when the materials were seeded with 1×10^6 donor BMSCs, bone formation in the defect was observed (Figure 3A- 4, 5, 6). While all materials showed bone formation in the presence of BMSCs, quantification of the radiopacity of each material, revealed significantly higher amounts of bone on the CA groups than the PLGA group ($p<0.001$) (Figure 3B). A two-fold increase in bone formation was observed on CA and CAc structures than the PLGA group.

3.3. Histological analysis of implanted scaffolds

There was little to no bone formation associated with the materials alone after 8 weeks post implantation in the calvarial defect (DIC -Figures S2). Additionally, a lack of robust bone mineral deposition was observed indicating low degrees of bone mineral deposition. The materials showed presence of cells in their interior along (DAPI -Blue stain, Figures S2) along with robust alkaline phosphatase (AP) staining, indicative of osteoblastic activity (AP -Red stain label Figures S2). However, the PLGA matrices had most of the cellularity (DAPI-blue) and ostoblastic activity (AP-red) confined to the periphery of the implant (Figure S2, C and I). Comparatively, cellularity (DAPI-blue) and ostoblastic activity (AP-

red) were seen well inside the scaffold interior and were more evenly distributed in the case of CA (Second row: Figure S2, D and O) and CAc (Figure S2, J and P). Finally, stronger osteoclastic activity was observed in CAc (Figure S2, L and R) than in PLGA (Figure S2, E and K). Thus, though the materials alone could not facilitate proper bone formation, cellularization, osteoblastic, and osteoclastic cellular activity of host cells were observed to be more active in CA and CAc than in PLGA implants, where this activity was confined mostly to the periphery of the materials. There was no significant difference between the test and the control materials in the quantity of cells or amount of osteoblast and osteoclast activity. However, more uniform distribution of cells, along with osteoblast and osteoclast activity, was observed on CA and CAc structures than the PLGA group.

3.4. ECM protein deposition by scaffolds and BMSCs

The collagen I (Coll I) and bone sialoprotein (BSP) content of scaffolds loaded with BMSCs was evaluated by immunostaining (Coll I-yellow, BSP-red). Both Coll I and BSP were found in all the sections. The BSP content was similar among the groups (First row in each panel of Figure 4). The distribution of collagen (Second row in each panel of Figure 4) was confined to certain areas in the case of PLGA thereby lacking a continuous collagenous extracellular matrix (ECM). Therefore, though collagen was present incomplete bridging was seen in the case of PLGA (Figure 4-C and G). The distribution of collagen was more uniform throughout the CA (Figure 4-D and K) and CAc (Figure 4-H and L) matrices. Moreover, collagen intensity, when contrasted to the host bone, was weaker in PLGA matrices (Figure 4-C vs the central insets in respective rows). The intensity of the collagen signal from CA (Figure 4-D and K vs the central inset in the rows) and CAc (Figure 4-H and L vs the central insets in the rows) matrices were comparable to the host bone. Quantitatively, the collagen content produced on CA and CAc matrices were double that of the collagen presented on the PLGA matrix (Figure 5B) ($p<0.001$).

3.5. Mineral deposition, host and donor cell participation in bone formation by materials along with BMSCs

All scaffolds seeded with BMSCs showed bone formation (DIC signal in Figure S3, Figure 6, and Figure S4) and new mineral deposition (AC-red signal in Figure S3, Figure 6, and Figure S4). Bone formation was confined to certain regions of the material in the case of PLGA (Figure S3-A, C, E, G; Figure 6-A, C, E, G), with minimal closure of the defect at the interphase of the calvarium and dura. Comparatively, on CA and CAc matrices, bone formation was well distributed and a good bone bridge was formed at the interphase of the calvarium and dura (CA-Figure S3-B, D, F, H; Figure S4-A, C, E, G; CAc-Figure 6-B, D, F, H; Figure S4-B, D, F, H).

Quantitatively, the bone area on CA and CAc was approximately double what was seen in PLGA implants (Figure 7A), however, there were no differences in the quantity of bone mineral deposition (Figure 7B), donor cells (Figure 7C) and host cells (Figure 7D) amongst all the groups. Additionally, all groups contained a higher presence of Col3.6-Cyan (donor) cells than the Col3.6tpz (host cells). The donor cells also presented better merger with new mineral deposition AC stain (red), (smaller insets in each of the insets of Figure S3, Figure 6, and Figure S4).

3.6. Osteoblastic and osteoclastic activity in Materials seeded with BMSCs

The cellular content (DAPI-blue) of the scaffolds was similar among PLGA, CA and CAc matrices (Figure 8). The AP (red) content was also similar between the groups (Figure 8). However, the distribution was more uniform and a continuous layer of cells with active AP content was seen in the case of CA and CAc. The PLGA materials showed cell (DAPI) and AP distribution in only pocket areas of the matrix. There was also a lack of continuous tissue (Figure 8-C and G) and osteoblastic AP activity at the interphase of the cranium and dura in the PLGA implants (Figure 8-A and E), while a good degree of tissue and ostoblastic activity was seen in analogous regions of CA (Cells-Figure 8-D and K; AP-Figure 8-B and I) and CAc (Cells-Figure 8-H and L; AP-Figure 8-F and J). Though osteoclastic bone resorption was not different among all the groups (Figure S5), the distribution of osteoclast activity, as indicated by TRAP staining, was more homogenous with CA (Figure S5-B, E) and CAc (Figure S5-D, F), than with PLGA matrices (Figure S5-A, C).

4. Discussion

Scaffold based bone tissue engineering relies on the ability of a temporary ECM to direct tissue healing in a desirable direction[32]. Synthetic polymers such as biodegradable polyesters, like polylactic acid (PLA), polyglycolic acid (PGA) and their copolymer (PLGA) provide a convenient material platform for the formulation of BTE scaffolds. However, clinical outcomes of long-term implantation of these materials, both in animal models and in human patients, have yielded variable results in bone healing. For instance, the formation of a sterile sinus over the site of implantation have been associated with polymeric implants with loss of mechanical stiffness occurring before bone healing is complete[33]. In another study, Biofix, a commercially available PGA implant, elicited high levels of immune (foreign body) reaction, along with moderate to severe osteolysis, as early as four to six weeks post implantation[34]. In a nine-year study of patients implanted with α-hydroxyl ester bone implants, foreign body reaction and osteoarthritis at the joints located in the vicinity of the implant were observed[35]. Inclusion of hydroxyapatite (HA) with poly-α-hydroxyl esters[36] to neutralize the degradation products have yielded greater bone mineralization in animal models. Even so, bone formation at the implant core, where acidic degradation products accumulate, remains a challenge[37]. Considering these limitations of synthetic polymers, natural polymers are an attractive alternative for BTE, providing greater biocompatibility and bioactivity[38].

Cellulose is the most abundant natural polymer in the biosphere and it is well suited for BTE due to its mechanical capability[18] and hydrophilic nature[20]. Several attempts have been made to employ cellulose in tissue engineering. Barbie *et al.* had conducted a 34-week implantation of cellulose into the femur of rabbits and observed a good degree of integration and minimal inflammatory reaction[39]. Cellulose and cellulose phosphate materials were also seen to support bone healing[40]. Yet, most studies that use cellulose for BTE do not take advantage of its strong mechanical property, as the materials formulated are often in the form of hydrogels[40, 41] or fiber mats[42] that cannot serve as a supportive matrix for bone regeneration.

Collagen, the most abundant protein in the animal kingdom[43], is another natural polymer and is the major protein component of bone[44]. Most BTE matrices that employ collagen, subject the collagen to extensive processing to maintain its physical stability, but doing so compromises the bioactivity of the collagen[45]. In our previous work we had established a cellulose acetate sintered microsphere system coated with nanofibrillar collagen, where the mechanical competence of cellulose that was in the mid-range of trabecular bone with a compressive modulus 266.75±33.22MPa and strength 12.15±2.23MPa[18, 19] and the bioactivity of collagen were preserved with a collagen nanofiber diameter of 75±7.0nm[20]. Human osteoblast[19] and human mesenchymal stem[20] cell attachment, survival, proliferation and osteoblastic differentiation on these materials were far superior to the responses observed on similar structured PLGA materials, *in vitro*.

Though, *in vitro* experiments can indicate the potential application for a biomaterial, implantation of the material into a functional defect and its performance in the body, where a number of other factors such as the systemic and local responses play a crucial role, ultimately determine the success of the implant. To test a biomaterial's ability to support bone formation in the body, its performance in a critical sized defect must be tested *in vivo*[46]. Here, in our studies we formulated a mechanically competent, 3D porous structure of cellulose acetate and collagen, and contrasted its performance with a model synthetic polymer (PLGA) for its ability to heal a critical sized bone defect. Our earlier study had demonstrated the ability of CA and CAc to induce the osteoblastic differentiation of seeded human mesenchymal stem cells (hMSCs) *in vitro*[20].

In the scaffold systems tested here, the morphology of the engineered PLGA and CA matrices were strikingly different. While PLGA showed very smooth surface and interfaces (Figure 2 G, J), CA matrices showed many surface undulations (Figure 2 H, K) revealing a rough surface morphology. The cellular response towards an implanted biomaterial depends on the physio-chemical properties of the biomaterial. Deligianni *et al.*, found that rough surfaces were more conducive for attachment and osteoblastic differentiation of BMSCs *in vitro*[47]. Lincks *et al.*, also found that titanium implants with rough surfaces may serve better for orthopaedic applications[48] and allow for greater osteointegration of the implant. It is also known that cells adhere onto materials by forming adhesions through a process similar to endocytosis. Rough surfaces induced greater endocytotic vesicle formation and actin cytoskeletal remodeling than smooth surfaces, favoring cell retention and proliferation on such surfaces[49]. Finally, it is also noted that protein adsorption and conformational presentation for cell-material, ligand-receptor interaction is greater on moderately rough substrates than smooth ones[50].

A remaining challenge of BTE implants is limited diffusion, which results in the accumulation of material degradation products at the implant core. Consequently, acidic byproducts, such as those associated with PLGA, can cause minimum cellularity at the scaffold core[8, 27, 51] resulting in bone formation that is limited to the periphery of the implant[28]. Our results have demonstrated that the natural polymer based CA and CAc 3D-porous micro and micro-nanostructures showed greater tissue infiltration in contrast to PLGA structures. Cellularity was confined to the periphery of synthetic PLGA implants (Figures S2). This can be attributed to higher biocompatible properties[52] of natural

polymeric materials in contrast to synthetic polymers that may have toxic byproducts[53] that accumulate in the interior of the matrix[54].

To increase the bioactivity of biomaterials, cells or other factors are added to attain better tissue healing responses. Limitations associated with growth factors, such as off-target effects like ectopic bone formation, as seen with bone morphogenetic protein-2 (BMP-2)[55] has prevented their wide spread clinical use. Small molecule drugs offer advantages, like ease of processing, however, these molecules may also have non-specific off-target effects[56]. Usage of autologous stem cells along with biomaterials is proving to be a more clinically viable option for enhancing bone defect healing. Hence in this study we tested the performance of a cellulose acetate-collagen, micro-nano structured BTE scaffold system, in a critical sized mouse calvarium defect in combination with bone marrow stromal cells. Host cells carried a green fluorescent collagen reporter, whereas donor BMSCs carried a cyan fluorescent collagen reporter. In this manner, the origin of new bone formation could be monitored histologically.

Clinical studies have shown that inclusion of autologous BMSCs in materials implanted into bone defects lead to accelerated defect bridging and functional limb recovery than the use of materials alone[57]. The accelerated healing of bone defects by combining autologous BMSCs with materials is also seen to occur in animal models like sheep[58] and dog[59]. While these results suggest that using BMSCs accelerates bone regeneration, the mechanism of bone regeneration by implanted BMSCs is still debated. It is seen that BMSCs when implanted can have the effect of reducing the levels of inflammatory cytokines such as IL-6 and IL-1β and TNF-α[60]. Also, studies where extracellular vesicles derived from BMSCs were delivered into bone defect showed improved bone regeneration[61], indicating that factors released by BMSCs may be responsible for stimulating the host cells to differentiate into an osteoblastic phenotype. BMSCs are capable of differentiating into osteoblastic lineage and hence could contribute directly towards bone regeneration in a defect[62], as well. Others studies have shown a reduction in the implanted cell population with time and hence a more paracrine mechanism of healing, where the implanted cells act as source of factors that signal regeneration by the host cells[63]. In the present study, with the inclusion of BMSCs along with the materials, it was observed that the number of donor cells far exceeded the number of host cells in all three materials tested (Figure 7 C, D, E). The donor cells (Cyan-blue signal) showed greater degree of localization with the newly deposited mineral (AC-red signal), while a relatively thin layer of host cells (Tpz-Green signal) can be seen in the same regions. These results indicate donor BMSCs played an active role in the formation of bone. Additionally, the donor cells may also have contributed indirectly to bone formation by signaling the host cells to enter the defect.

Natural polymeric materials presented a rough morphology, greater hydrophilicity and chemical functionalities that resemble the natural ECM of bone. These are in sharp contrast to the smooth morphology, highly hydrophobic nature and progressive deposition of acidic degradation products presented by polyester based materials. Even in the absence of cells, the CA materials showed a greater degree of cell infiltration in contrast to PLGA (Figure S2). The natural polymers allowed the host cells to perfuse through them and facilitated an equal distribution in the interior of the scaffold due to the greater biocompatibility and

biomimetic nature of the material. PLGA, on the other hand did not allow such a high degree of cellular infiltration. The degradation products at the core of the material are less conducive for achieving a uniform cell infiltration. Therefore, bone formation (DIC channel) and new mineral deposition (AC-red channel) was widely distributed throughout the material in CA and CAc groups (DIC, and AC-red channels in Figures 6, Figures S3, and S4), whereas an uneven distribution was observed on PLGA implants.

When equal number of donor BMSCs were implanted along with the materials, the natural polymers allowed for uniform cell adhesion on all parts of the material. On the other hand, PLGA facilitated a more skewed distribution of cells. Also, the fraction of scaffold covered by bone was significantly higher in the natural polymers (CA and CAc) than PLGA (Figure 7A). The radiopacity of the defect revealed a two-fold increase in bone formation with CA and CAc matrices when compared to PLGA (Figure 3). Further, collagen content and staining intensity were greater and better distributed on the natural microstructures than PLGA (Figures 4 and 5B). The CA and CAc materials also lead to bone formation across the defect at the interface of dura and the calvarium, which was absent in the PLGA treated groups. The differences in BMSC-material interactions were important factors in determining the quality of the regenerated bone in the defects. Additionally, the lack of growth inhibitory degradation products on natural polymers leads to better BMSC performance. These advantages of natural polymer over synthetic polymer translated into greater collagen production by the implanted BMSCs and greater density of regenerated bone on the natural polymers.

Cellulosic scaffolds were coated with collagen (CAc) to increase the innate bioactivity of the material[64]. Type 1 collagen self-assembled into nanofibers on the CA microspheres creating a nanofibrillar bone-ECM component[19]. Previous *in vitro* data showed greater bone formation with collagen coated scaffolds[20]. At 8-weeks after implantation into a critical sized bone defect, no significant differences were found between CA and CAc, in terms of quantity or quality of the regenerated bone. This may be due to the degradation of the collagen from the matrix at an earlier time point than observed *in vitro*. The collagen coating may help achieve biocompatibility and cellularization of the implant at an earlier stage than its uncoated counterpart. After an extended period of time, there may be little difference between the collagen coated and uncoated CA porous micro-nanostructures[20]. A technique to improve the retainment of collagen on the matrix, such as chemical conjugation, may be necessary to observe the prolonged benefits of prolonged nanofiber bioactivity[65].

Several limitations assoicated with the study include the lack of While all the animals were randomly assigned to the study groups, following guidelines like ARRIVE for randomization and blinding of the samples, as described in the ARRIVE guidelines. Randomization and blinding oft the study samples would strengthen the results. Additonally, the mice used in the studies with no cells were female, whereas studies with cells were male. However, the mice used in the study were juvenille in age (10-12 weeks). Strube *et. al.*[66], noticed differences in bone healing between female and male rodents did not occur until 12 months of age (elderly mice). Since no definitive evidence for differential bone healing in

juvenile mice exists, we believe any impact from sex differences on bone regeneration would be minimal in our studies.

Our results indicate that cellulose based materials, when designed to possess the desirable characteristics of surface roughness, hydrophilicity, porosity and mechanical competence may be better suited for bone regeneration than conventional synthetic polymer matrices. We found donor cells to be indispensable for proper bone formation to occur on the micro-nanostructured matrices. The scaffold carrier can accelerate BMSC mediated bone regeneration to a greater or lesser extend depending on its material properties. This opens the possibility for increased use of cellulose-based structures in BTE applications on a wider scale.

5. Conclusions

In summary, we conclude that natural polymeric CA based 3D porous microstructures performed better than well-established synthetic PLGA matrices of similar dimensions, in inducing healing of critical sized bone defects. The CA based materials allowed better cellular infiltration and better distribution of cellular activity. The addition of BMSCs enhanced bone and collagen formation by two-fold on natural materials than PLGA, indicating a higher density and quality of regenerated bone. No significant difference in bone formation was found with the inclusion of collagen nanofibers (CAc) when compared to neat CA scaffolds, as was observed previously with in vitro studies[67]. This observation may be due to degradation of collagen at a faster rate than what is seen in vitro, and hence the effects of nanofibrillar collagen were negligible after 8 weeks of implantation. Finally, donor BMSCs were found in regions of new mineral deposition along with fewer host BMSCs suggesting donor BMSCs may have played a critical role in the formation of new bone by directly depositing matrix and/or indirectly signaling host BMSCs to contribute to the process. Though there were no differences in the amount of donor BMSCs retained by the materials, a more uniform cellular distribution was found on the natural polymers than on the synthetic polymer. This study supports the use of natural polymeric 3D-porous microstructures of cellulose, in combination with donor derived BMSCs, to effectively induce bone formation. Natural based matrices may be an effective alternative to synthetic polymer based BTE matrices.

Supplementary Material

Refer to Web version on PubMed Central for supplementary material.

Acknowledgments

These studies were supported by funding support from the National Institute of Biomedical Imaging and Bioengineering of the National Institutes of Health (Award Number R01EB020640), the National Science Foundation (IIP-1311907 and IIP-1355327), as well as the Connecticut Regenerative Medicine Research Fund (15-RMB-UCHC-08).

References

1. Campana V, Milano G, Pagano E, Barba M, Cicione C, Salonna G, Lattanzi W, Logroscino G. Journal of Materials Science: Materials in Medicine. 2014; 25:2445. [PubMed: 24865980] Greenwald AS, Boden SD, Goldberg VM, Khan Y, Laurencin CT, Rosier RN. The Journal of Bone & Joint Surgery. 2001; 83:S98.Finkemeier CG. J Bone Joint Surg Am. 2002; 84:454. [PubMed: 11886919] Faour O, Dimitriou R, Cousins CA, Giannoudis PV. Injury. 2011; 42:S87. [PubMed: 21723553]
2. Amini AR, Laurencin CT, Nukavarapu SP. Critical Reviews™ in Biomedical Engineering. 2012; 40
3. Bose S, Roy M, Bandyopadhyay A. Trends in biotechnology. 2012; 30:546. [PubMed: 22939815]
4. Bacakova L, Filova E, Parizek M, Ruml T, Svorcik V. Biotechnology advances. 2011; 29:739. [PubMed: 21821113]
5. Lampin M, Warocquier-Clérout R, Legris C, Degrange M, Sigot-Luizard M. Journal of biomedical materials research. 1997; 36:99. [PubMed: 9212394]
6. Reilly GC, Engler AJ. Journal of biomechanics. 2010; 43:55. [PubMed: 19800626]
7. Gentile P, Chiono V, Carmagnola I, Hatton PV. International journal of molecular sciences. 2014; 15:3640. [PubMed: 24590126]
8. Anderson JM, Shive MS. Advanced drug delivery reviews. 2012; 64:72.
9. Gunatillake PA, Adhikari R. Eur Cell Mater. 2003; 5:1. [PubMed: 14562275]
10. Mano J, Silva G, Azevedo HS, Malafaya P, Sousa R, Silva S, Boesel L, Oliveira JM, Santos T, Marques A. Journal of the Royal Society Interface. 2007; 4:999.
11. Valmikinathan CM, Mukhatyar VJ, Jain A, Karumbaiah L, Dasari M, Bellamkonda RV. Soft Matter. 2012; 8:1964.
12. Arias JL, Fernández MaS. Chemical Reviews. 2008; 108:4475. [PubMed: 18652513]
13. Jiang T, Abdel-Fattah WI, Laurencin CT. Biomaterials. 2006; 27:4894. [PubMed: 16762408] Jiang T, Kumbar SG, Nair LS, Laurencin CT. Current topics in medicinal chemistry. 2008; 8:354. [PubMed: 18393897]
14. Aravamudhan A, Ramos DM, Nada AA, Kumbar SG. Natural and Synthetic Biomedical Polymers. 2014; 67
15. Arpornmaeklong P, Pripatnanont P, Suwatwirote N. International journal of oral and maxillofacial surgery. 2008; 37:357. [PubMed: 18272341] Geissler U, Hempel U, Wolf C, Scharnweber D, Worch H, Wenzel KW. Journal of biomedical materials research. 2000; 51:752. [PubMed: 10880125]
16. Valmikinathan CM, Defroda S, Yu X. Biomacromolecules. 2009; 10:1084. [PubMed: 19323510]
17. Yao C, Gao F, Chen Y, Miao X, Zhou Y, Shao D. Chinese journal of reparative and reconstructive surgery. 2011; 25:1481. [PubMed: 22242351] Casper CL, Yang W, Farach-Carson MC, Rabolt JF. Biomacromolecules. 2007; 8:1116. [PubMed: 17326680] Duan Y, Wang Z, Yan W, Wang S, Zhang S, Jia J. Journal of Biomaterials Science, Polymer Edition. 2007; 18:1153. [PubMed: 17931505]
18. Kumbar S, Toti U, Deng M, James R, Laurencin C, Aravamudhan A, Harmon M, Ramos D. Biomedical Materials. 2011; 6:065005. [PubMed: 22089383]
19. Aravamudhan A, Ramos DM, Nip J, Harmon MD, James R, Deng M, Laurencin CT, Yu X, Kumbar SG. Journal of biomedical nanotechnology. 2013; 9:719. [PubMed: 23621034]
20. Aravamudhan A, Ramos D, Jenkins N, Dyment N, Sanders M, Rowe D, Kumbar S. RSC Advances. 2016; 6:80851.
21. Cowan CM, Shi YY, Aalami OO, Chou YF, Mari C, Thomas R, Quarto N, Contag CH, Wu B, Longaker MT. Nature biotechnology. 2004; 22:560.
22. Gohil SV, Adams DJ, Maye P, Rowe DW, Nair LS. Journal of Biomedical Materials Research Part A. 2014; 102:4568. [PubMed: 24677665] Yamamoto M, Takahashi Y, Tabata Y. Biomaterials. 2003; 24:4375. [PubMed: 12922150]
23. Gómez-Barrena E, Rosset P, Müller I, Giordano R, Bunu C, Layrolle P, Konttinen YT, Luyten FP. Journal of cellular and molecular medicine. 2011; 15:1266. [PubMed: 21251219] Horwitz EM, Prockop DJ, Fitzpatrick LA, Koo WW, Gordon PL, Neel M, Sussman M, Orchard P, Marx JC,

Pyeritz RE. Nature medicine. 1999; 5:309.Bianco P, Cao X, Frenette PS, Mao JJ, Robey PG, Simmons PJ, Wang C-Y. Nature medicine. 2013; 19:35.

24. Martino S, D'Angelo F, Armentano I, Kenny JM, Orlacchio A. Biotechnology advances. 2012; 30:338. [PubMed: 21740963] Beitzel K, McCarthy MB, Cote MP, Russell RP, Apostolakos J, Ramos DM, Kumbar SG, Imhoff AB, Arciero RA, Mazzocca AD. Arthroscopy: The Journal of Arthroscopic & Related Surgery. 2014; 30:289. [PubMed: 24581253] Discher DE, Mooney DJ, Zandstra PW. Science. 2009; 324:1673. [PubMed: 19556500] Giancotti FG, Ruoslahti E. Science. 1999; 285:1028. [PubMed: 10446041]
25. Yu X, Xia Z, Wang L, Peng F, Jiang X, Huang J, Rowe D, Wei M. Journal of Materials Chemistry. 2012; 22:9721.
26. Curran JM, Chen R, Hunt JA. Biomaterials. 2006; 27:4783. [PubMed: 16735063] Benoit DS, Schwartz MP, Durney AR, Anseth KS. Nature materials. 2008; 7:816. [PubMed: 18724374] Yim EK, Darling EM, Kulangara K, Guilak F, Leong KW. Biomaterials. 2010; 31:1299. [PubMed: 19879643] Engler AJ, Sen S, Sweeney HL, Discher DE. Cell. 2006; 126:677. [PubMed: 16923388] Kasten P, Beyen I, Niemeyer P, Luginbühl R, Bohner M, Richter W. Acta iomaterialia. 2008; 4:1904.Murphy CM, Haugh MG, O'Brien FJ. Biomaterials. 2010; 31:461. [PubMed: 19819008]
27. Amini AR, Adams DJ, Laurencin CT, Nukavarapu SP. Tissue Engineering Part A. 2012; 18:1376. [PubMed: 22401817]
28. Jiang T, Nukavarapu SP, Deng M, Jabbarzadeh E, Kofron MD, Doty SB, Abdel-Fattah WI, Laurencin CT. Acta biomaterialia. 2010; 6:3457. [PubMed: 20307694]
29. Kalajzic I, Kalajzic Z, Kaliterna M, Gronowicz G, Clark S, Lichtler A, Rowe D. Journal of Bone and Mineral Research. 2002; 17:15. [PubMed: 11771662] Bilic-Curcic I, Kronenberg M, Jiang X, Bellizzi J, Mina M, Marijanovic I, Gardiner E, Rowe D. Genesis. 2005; 43:87. [PubMed: 16149065]
30. Wang YH, Liu Y, Buhl K, Rowe DW. Journal of Bone and Mineral Research. 2005; 20:5. [PubMed: 15619664]
31. Liu Y, Wang L, Fatahi R, Kronenberg M, Kalajzic I, Rowe D, Li Y, Maye P. Bone. 2010; 47:916. [PubMed: 20673822]
32. Lutolf M, Hubbell J. Nature biotechnology. 2005; 23:47.
33. Hofmann G. Archives of orthopaedic and trauma surgery. 1995; 114:123. [PubMed: 7619632]
34. Weiler A, Helling HJ, Kirch U, Zirbes TK, Rehm KE. Bone & Joint Journal. 1996; 78:369.
35. Böstman O. Bone & Joint Journal. 1998; 80:333.
36. Shalumon K, Sheu C, Fong YT, Liao HT, Chen JP. Polymers. 2016; 8:429.
37. Zhang P, Hong Z, Yu T, Chen X, Jing X. Biomaterials. 2009; 30:58. [PubMed: 18838160]
38. Aravamudhan A, Ramos D, Nada A, Kumbar S. Natural and Synthetic Biomedical Polymers. 2014; 67
39. Barbie C, Chauveaux D, Barthe X, Baquey C, Poustis J. Clinical materials. 1990; 5:251. [PubMed: 10171537]
40. Fricain J, Granja P, Barbosa M, De Jéso B, Barthe N, Baquey C. Biomaterials. 2002; 23:971. [PubMed: 11791931]
41. Song SH, Yun YP, Kim HJ, Park K, Kim SE, Song HR. BioMed research international. 2014; 2014
42. Märtson M, Viljanto J, Hurme T, Saukko P. European surgical research. 1998; 30:426. [PubMed: 9838236]
43. Shoulders MD, Raines RT. Annual review of biochemistry. 2009; 78:929.
44. Viguet-Carrin S, Garnero P, Delmas P. Osteoporosis International. 2006; 17:319. [PubMed: 16341622]
45. Wahl DA, Sachlos E, Liu C, Czernuszka JT. Journal of Materials Science: Materials in Medicine. 2007; 18:201. [PubMed: 17323151]
46. Honda H, Tamai N, Naka N, Yoshikawa H, Myoui A. Journal of Artificial Organs. 2013; 16:305. [PubMed: 23700004]
47. Deligianni DD, Katsala ND, Koutsoukos PG, Missirlis YF. Biomaterials. 2000; 22:87.

48. Lincks J, Boyan B, Blanchard C, Lohmann C, Liu Y, Cochran D, Dean D, Schwartz Z. Biomaterials. 1998; 19:2219. [PubMed: 9884063]

49. Dalby MJ, Gadegaard N, Tare R, Andar A, Riehle MO, Herzyk P, Wilkinson CD, Oreffo RO. Nature materials. 2007; 6:997. [PubMed: 17891143] Dalby MJ, Berry CC, Riehle MO, Sutherland DS, Agheli H, Curtis AS. Experimental cell research. 2004; 295:387. [PubMed: 15093738]

50. Denis FA, Hanarp P, Sutherland DS, Gold J, Mustin C, Rouxhet PG, Dufrêne YF. Langmuir. 2002; 18:819.

51. Amini AR, Xu TO, Chidambaram RM, Nukavarapu SP. Tissue Engineering Part A. 2016; 22:610. [PubMed: 26914219]

52. Dang JM, Leong KW. Advanced drug delivery reviews. 2006; 58:487. [PubMed: 16762443]

53. Bostman O, Paivarinta U, Manninen M, Rokkanen P. Acta Orthopaedica Scandinavica. 1992; 63:555. [PubMed: 1332417]

54. von Burkersroda F, Schedl L, Göpferich A. Biomaterials. 2002; 23:4221. [PubMed: 12194525]

55. Tannoury CA, An HS. The Spine Journal. 2014; 14:552. [PubMed: 24412416]

56. Aravamudhan A, Ramos DM, Nip J, Subramanian A, James R, Harmon MD, Yu X, Kumbar SG. Current pharmaceutical design. 2013; 19:3420. [PubMed: 23432678]

57. Quarto R, Mastrogiacomo M, Cancedda R, Kutepov SM, Mukhachev V, Lavroukov A, Kon E, Marcacci M. New England Journal of Medicine. 2001; 344:385. [PubMed: 11195802]

58. Kon E, Muraglia A, Corsi A, Bianco P, Marcacci M, Martin I, Boyde A, Ruspantini I, Chistolini P, Rocca M. Journal of biomedical materials research. 2000; 49:328. [PubMed: 10602065] Shang Q, Wang Z, Liu W, Shi Y, Cui L, Cao Y. Journal of Craniofacial Surgery. 2001; 12:586. [PubMed: 11711828]

59. Yuan J, Cui L, Zhang WJ, Liu W, Cao Y. Biomaterials. 2007; 28:1005. [PubMed: 17092556]

60. Granero-Moltó F, Weis JA, Miga MI, Landis B, Myers TJ, O'Rear L, Longobardi L, Jansen ED, Mortlock DP, Spagnoli A. Stem cells. 2009; 27:1887. [PubMed: 19544445]

61. Qin Y, Wang L, Gao Z, Chen G, Zhang C. Scientific reports. 2016; 6

62. Deans RJ, Moseley AB. Experimental hematology. 2000; 28:875. [PubMed: 10989188]

63. Gnecchi M, Zhang Z, Ni A, Dzau VJ. Circulation research. 2008; 103:1204. [PubMed: 19028920]

64. Liu LS, Thompson AY, Heidaran MA, Poser JW, Spiro RC. Biomaterials. 1999; 20:1097. [PubMed: 10382825] Ferreira AM, Gentile P, Chiono V, Ciardelli G. Acta biomaterialia. 2012; 8:3191. [PubMed: 22705634]

65. Weadock K, Olson RM, Silver FH. Biomaterials, medical devices, and artificial organs. 1983; 11:293.

66. Strube P, Mehta M, Baerenwaldt A, Trippens J, Wilson CJ, Ode A, Perka C, Duda GN, Kasper G. Bone. 2009; 45:1065. [PubMed: 19679210]

67. Abdel-Fattah WI, Jiang T, El-Bassyouni GET, Laurencin CT. Acta Biomaterialia. 2007; 3:503. [PubMed: 17320493]

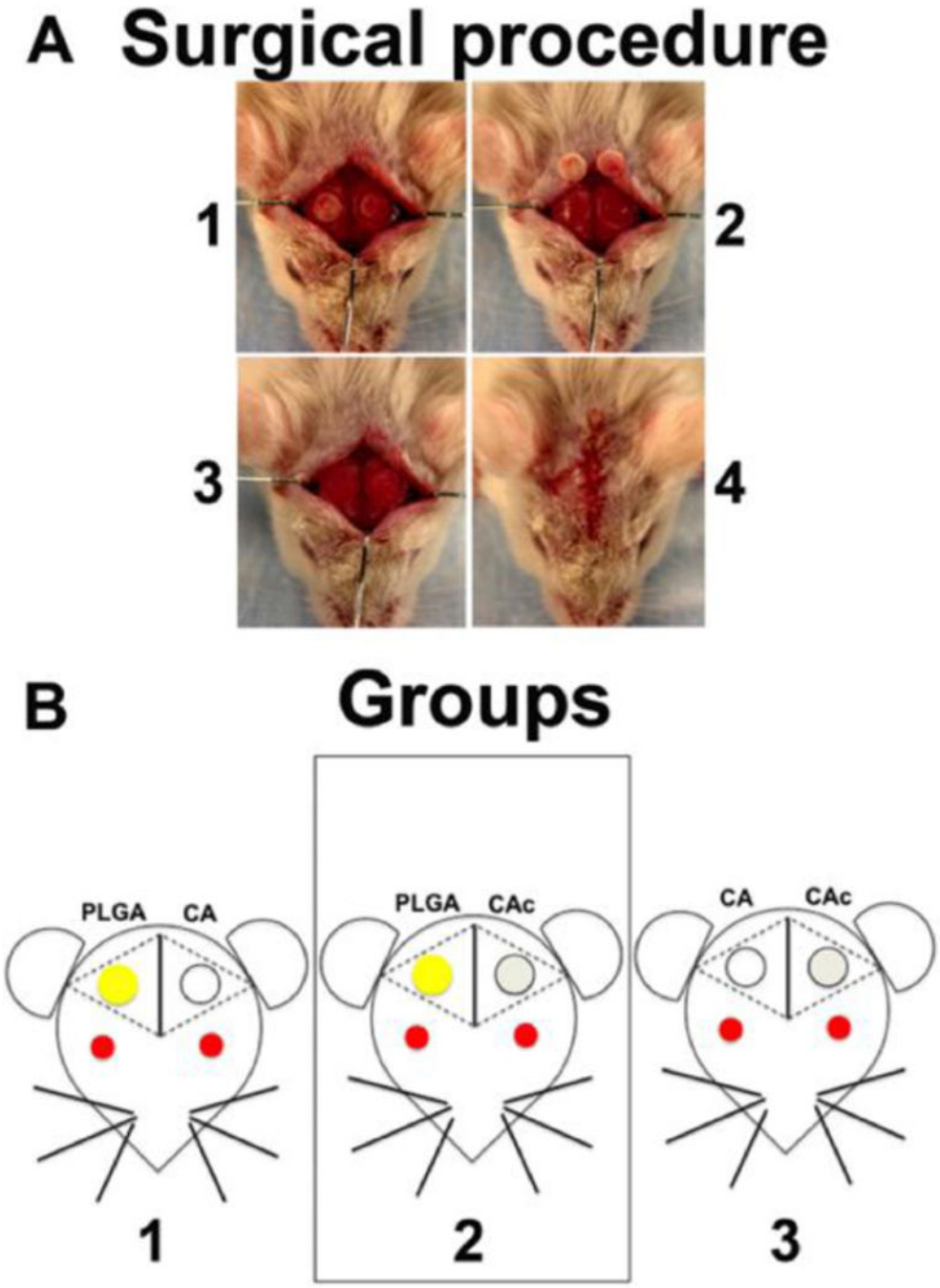

Figure 1. Surgical procedure and schematic of the study groups

(A) Steps in the surgical implantation: (1) Creation of two circular 3.5mm defects on the two sides of mouse calvaria, (2) removal of calvarial bone, (3) Implantation of the scaffolds into the defects, (4) Closure of the implants by suturing the skin. (B) Groups 1: left side defect was filled with PLGA and the right side defect with CA, group 2: left side defect was filled with PLGA and the right side was filled with CAc, group 3: left side was filled with CA and the right side was filled with CAc. In study 1, the materials alone were used. In study 2,

1×10^6 Col3.6-Cyan BMSCs from donor mice were seeded on to each scaffold before implantation into host mice with Col3.6-Tpz BMSCs.

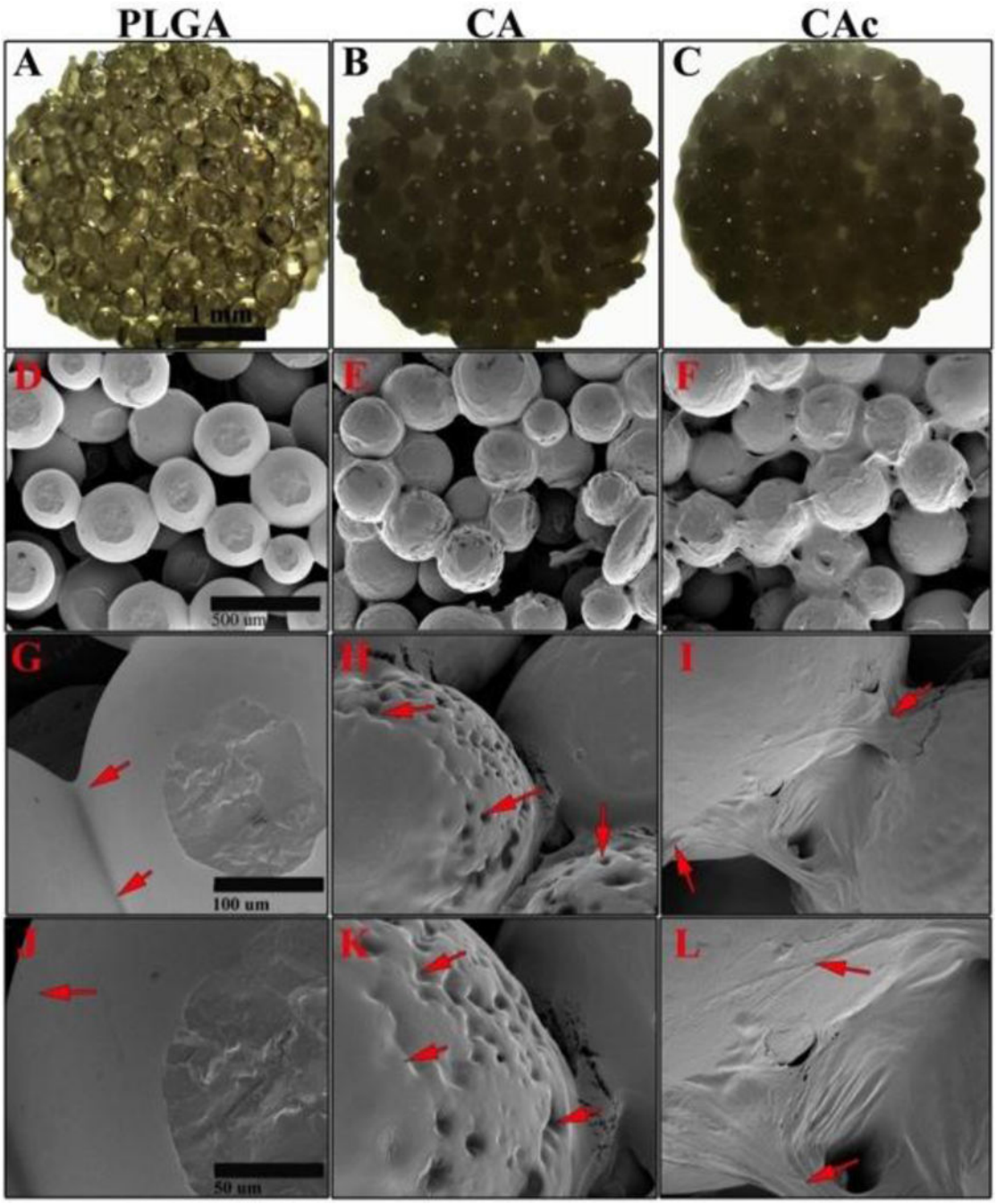

Figure 2. Examination of scaffold structure

Photographic images of 3D microporous scaffolds used (A) PLGA, (B) CA, (C) CAc, scale bar= 1mm; SEM images at 100× magnification (D) PLGA, (E) CA, (F) CAc, scale bar= 500μm; SEM images at 500× magnification (G) PLGA, (H) CA, (I) CAc, scale bar= 100μm; SEM images at 1000× magnification (J) PLGA, (K) CA, (L) CAc, scale bar= 50μm.

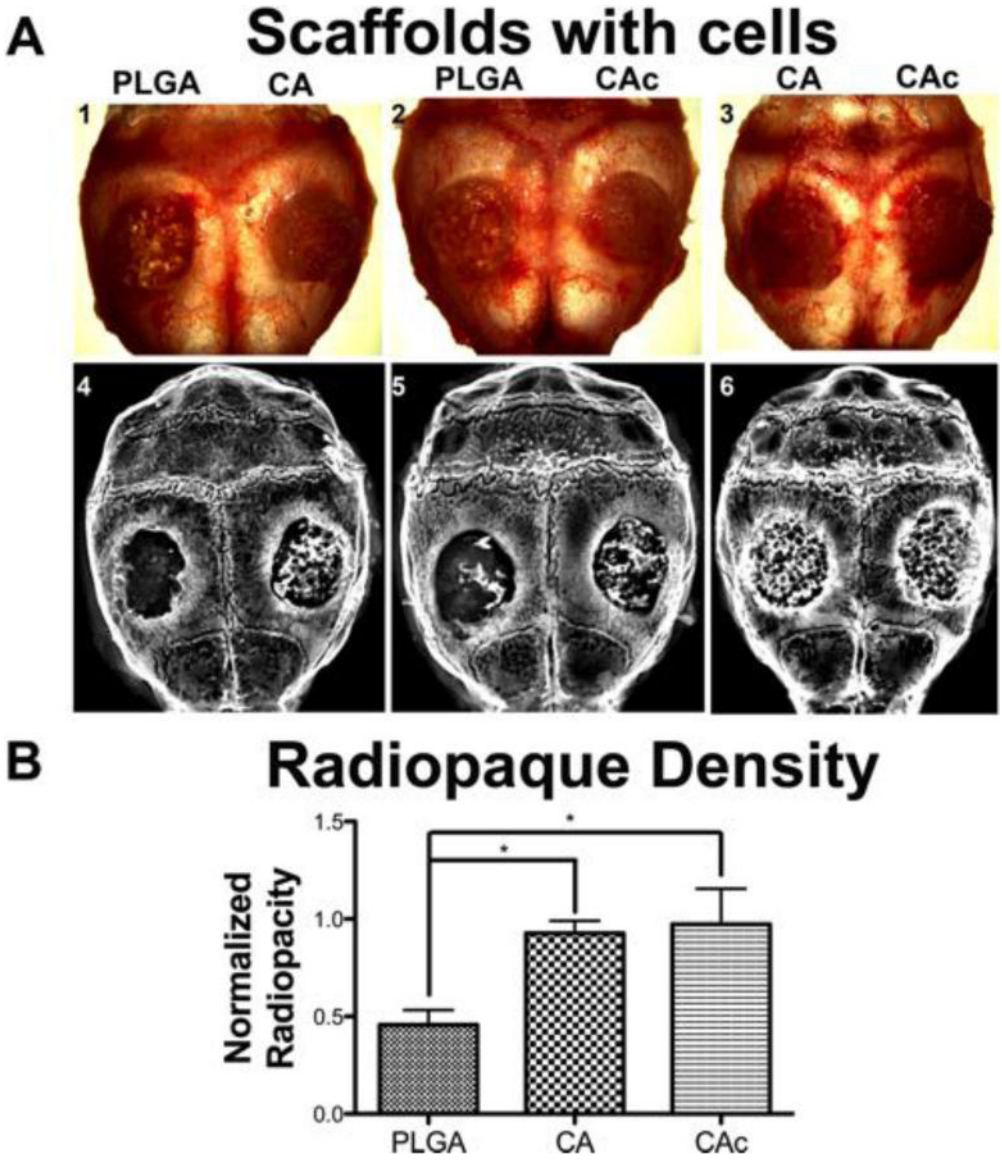

Figure 3. Whole calvaria and X-ray radiograph of defects implanted with materials and cells

(A) Top panel: 1. Group 1-PLGA vs CA, 2. Group 2-PLGA vs CAc, 3. Group 3-CA vs CAc.; X-ray radiographs of 4. Group 1-PLGA vs CA, 5. Group 2-PLGA vs CAc, 6. Group 3-CA vs CAc. (B) Quantitative radio opacity of defect area normalized to radio opacity of host bone, both measured per unit area; PLGA, n=6; CA, n=6; CAc, n=7. One-way ANOVAwith Tukey post-test, with 95% confidence intervals, *P < 0.001.

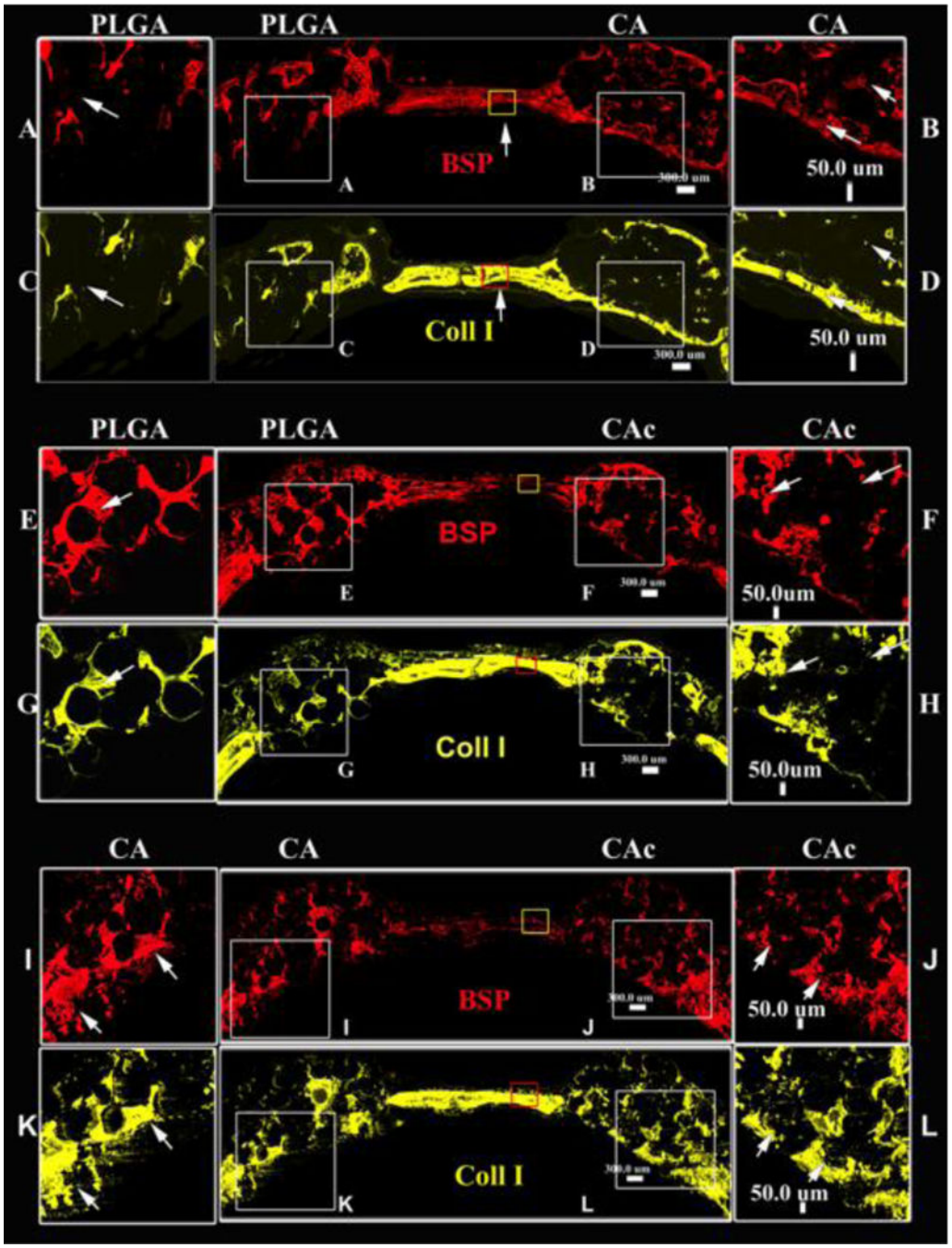

Figure 4. Deposition of ECM proteins with implantation of materials with donor cells

Fluorescent histological cross sectional images of calvaria implanted with material and cells at 8 weeks, A-D-Group 1, PLGA vs CA; E-H-Group 2, PLGA vs CAc; I-L-Group 3, CA vs CAc; Bone Sialoprotein (BSP) (red), Collagen 1 (yellow) –Bone ECM proteins.

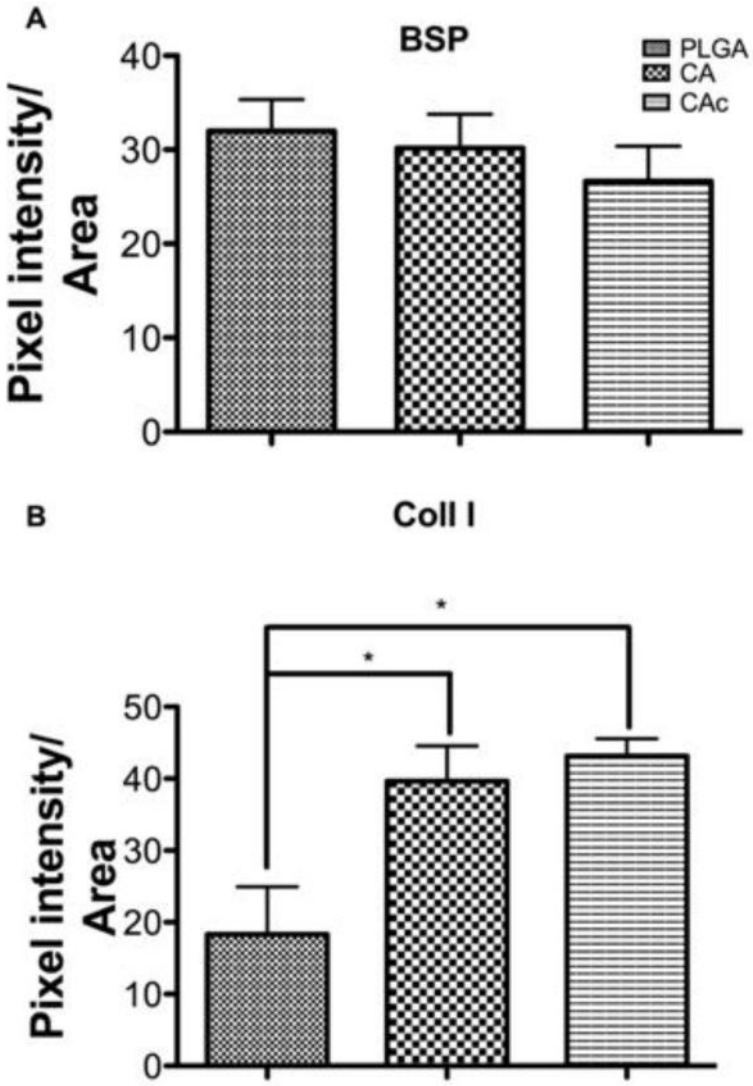

Figure 5. Quantification of Bone Sialoprotein (BSP) and Collagen I (Coll 1) deposited by materials with cells

(A) BSP-Bone sialoprotein (red stain in Figure 4), (B) Coll 1-Collagen 1 (yellow stain in Figure 4). One-way ANOVAwith Tukey post-test, with 95% confidence intervals, *P < 0.001.

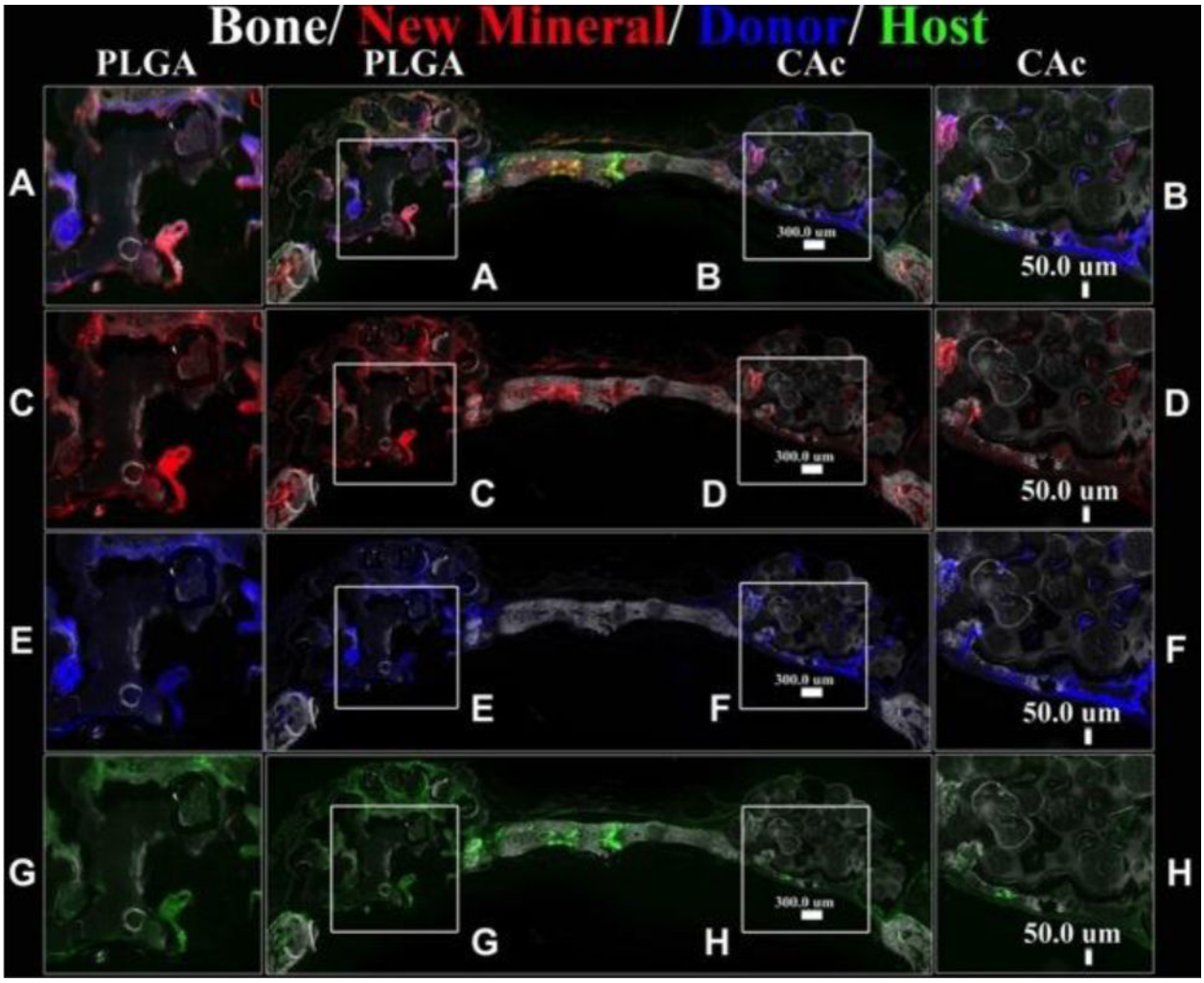

Figure 6. Fluorescent histological images of calvaria implanted with material and BMSCs at 8 weeks

Group 2: PLGA vs CAc, Top row: DIC-Differential interference channel image to visualize bone and microspheres with AC-red labeled alizarin complexone marking new mineral deposition, Donor cells-Col3.6-Cyan (blue), Host cells-Col3.6-Tpz (green) (PLGA inset A, CAc inset B); Second row: DIC-Differential interference channel image to visualize bone and microspheres with AC-red labeled alizarin complexone marking new mineral deposition (PLGA inset C, CAc inset D). Third row: DIC-Differential interference channel image to visualize bone and microspheres with Donor cells-Col3.6-Cyan (blue) (PLGA inset E, CAc inset F). Fourth row: DIC-Differential interference channel image to visualize bone and microspheres with Host cells-Col3.6-Tpz (green) (PLGA inset G, CAc inset H).

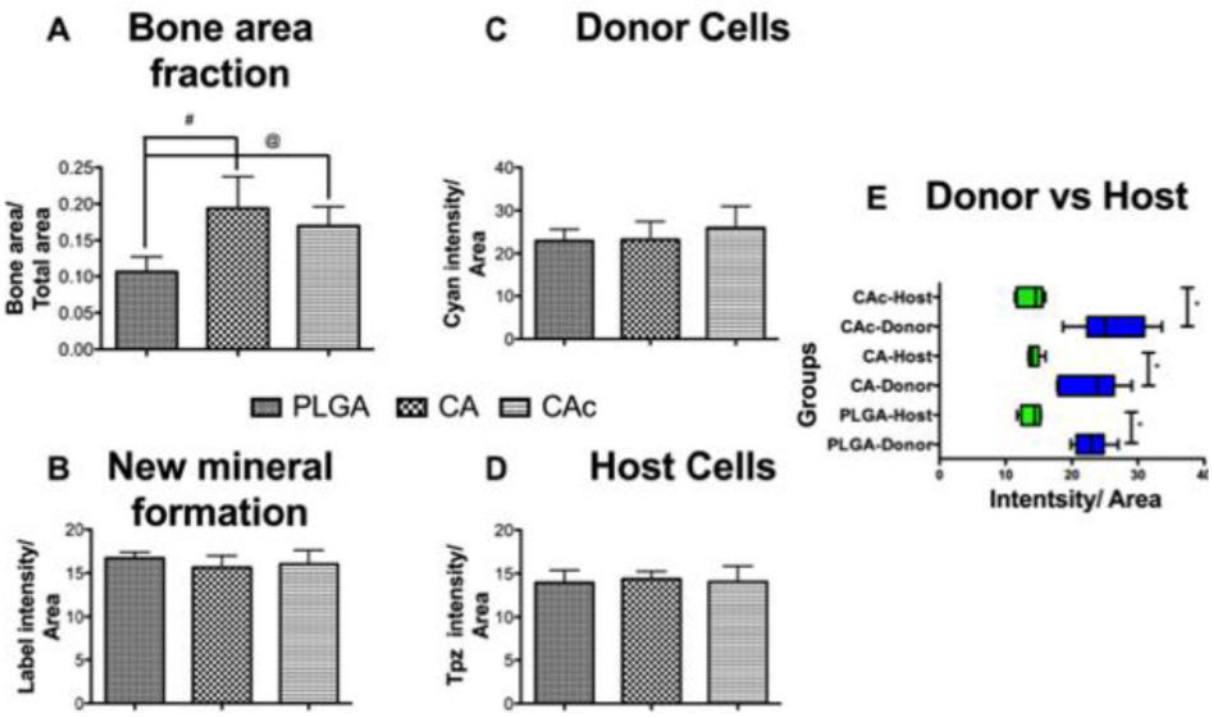

Figure 7. Quantification of Bone defect closure, mineralization and number of host and donor cells

(A) Bone area fraction-DIC quantification, (B) New mineral formation-AC quantification, (C) Donor cells-Col3.6-Cyan quantification, (D) Host cells-Col3.6-Tpz quantification, (E) Host (Green bars) and Donor (Blue bars) cells in each scaffold group. One-way ANOVAwith Tukey post-test, with 95% confidence intervals, *P < 0.001, #P < 0.01, @P < 0.05.

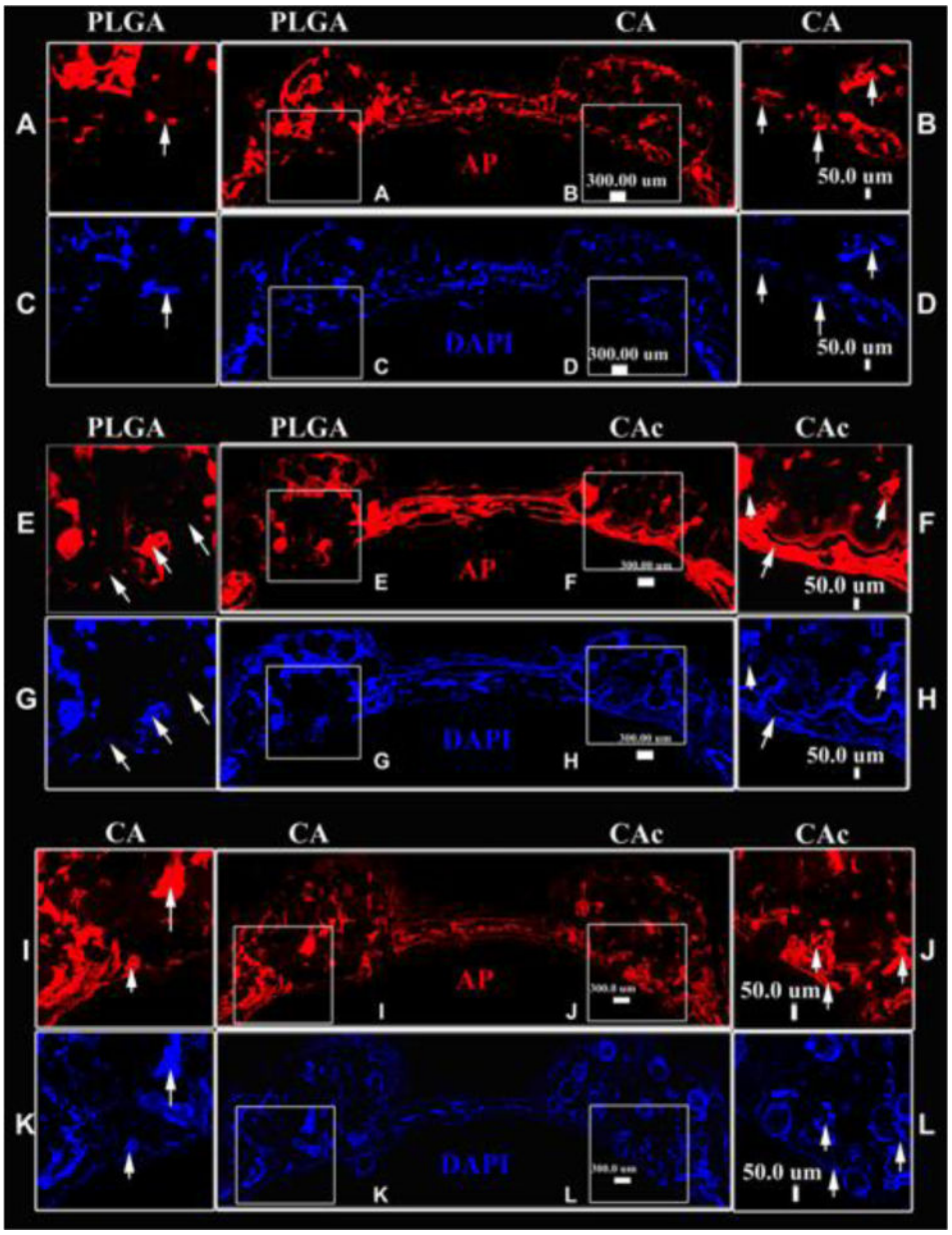

Figure 8. Fluorescent histological images of osteoblastic activity and cellularity on the calvaria implanted with material and BMSCs at 8 weeks

In each image set, First row: AP (red)-Alkaline phosphatase activity for osteoblastic activity. Second row : DAPI (blue) -cell nuclei. A-D-Group 1, PLGA vs CA (PLGA-inset A, C; CA -inset B, D); E-H-Group 2, PLGA vs CAc (PLGA –inset E. G; CAc –inset F, H); M-R-Group 3, CA vs CAc (CA –inset I, K; CAc –inset J, L).

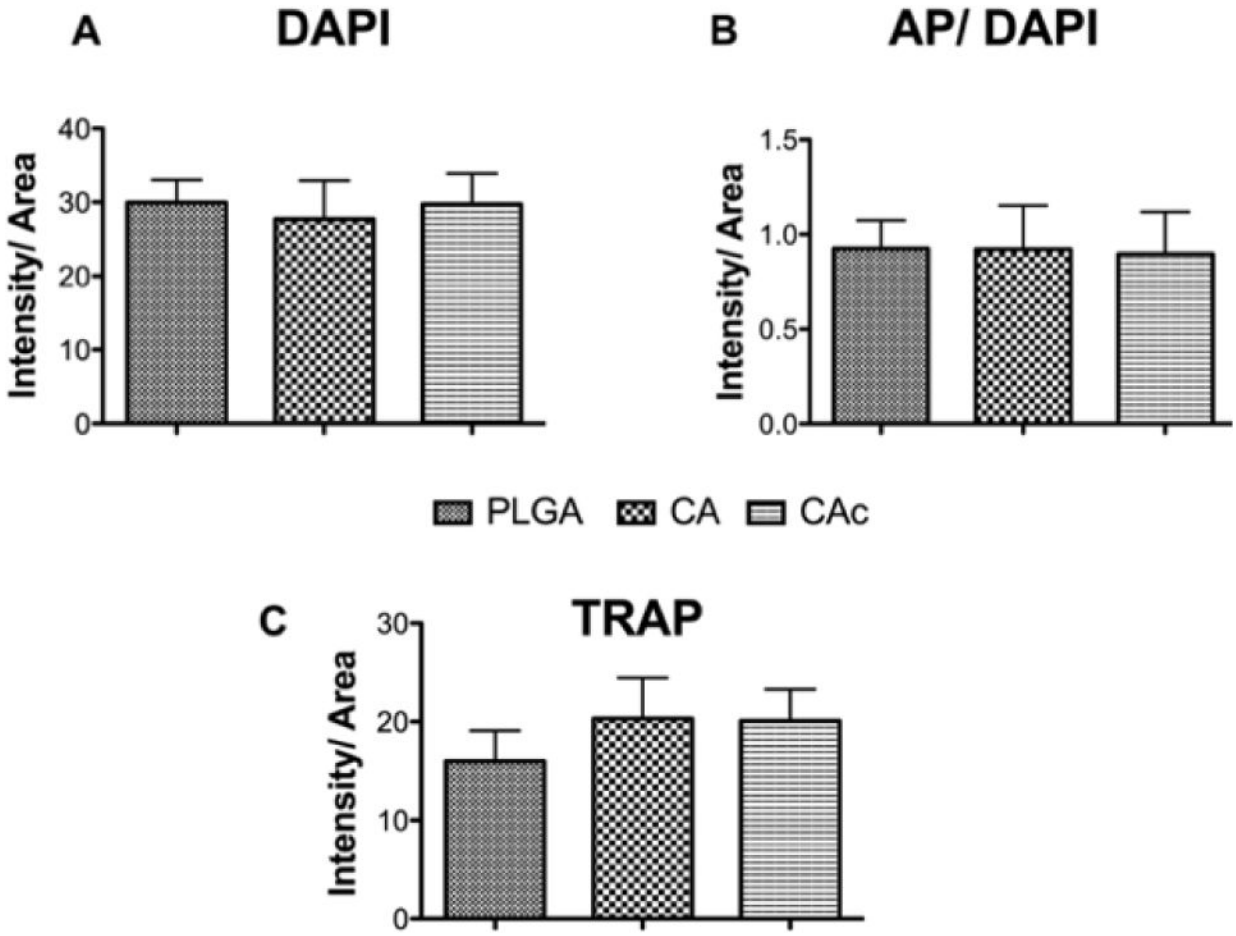

Figure 9. Quantification of Cellularity, osteoblastic and osteoclastic activity on the calvaria implanted with material and BMSCs at 8 weeks

(A) DAPI-cells, (B) AP/DAPI-osteoblastic activity, (C) TRAP-osteoclastic activity.